Neuron, Vol. 34, 961–972, June 13, 2002, Copyright ©2002 by Cell Press

Drosophila Fragile X Protein, DFXR, Regulates Neuronal Morphology and Function in the Brain

Joannella Morales,[1] P. Robin Hiesinger,[1] Andrew J. Schroeder,[3] Kazuhiko Kume,[3] Patrik Verstreken,[2] F. Rob Jackson,[3] David L. Nelson,[1] and Bassem A. Hassan[1,4,5]
[1]Department of Molecular and Human Genetics
[2]Program in Developmental Biology
Baylor College of Medicine
Houston, Texas 77030
[3]Department of Neuroscience
Tufts University School of Medicine
Boston, Massachusetts 02111
[4]Laboratory of Neurogenetics
Center for Human Genetics
Flanders Interuniversity Institute
for Biotechnology (VIB)
3000 Leuven
Belgium

Summary

Mental retardation is a pervasive societal problem, 25 times more common than blindness for example. Fragile X syndrome, the most common form of inherited mental retardation, is caused by mutations in the *FMR1* gene. Fragile X patients display neurite morphology defects in the brain, suggesting that this may be the basis of their mental retardation. *Drosophila* contains a single homolog of FMR1, *dfxr* (also called *dfmr1*). We analyzed the role of *dfxr* in neurite development in three distinct neuronal classes. We find that DFXR is required for normal neurite extension, guidance, and branching. *dfxr* mutants also display strong eclosion failure and circadian rhythm defects. Interestingly, distinct neuronal cell types show different phenotypes, suggesting that *dfxr* differentially regulates diverse targets in the brain.

Introduction

More than 500 genetic disorders are associated with mental retardation and most of these disorders are not understood in molecular terms. One of the most significant challenges in addressing the molecular mechanisms of mental retardation disorders is the difficulty of establishing animal model systems. Yet without such models, it will be difficult to understand the genetic pathways and molecular mechanisms underlying mental retardation. In a few instances, human homologs of *Drosophila* genes have been mapped to chromosomal intervals containing genes relevant to mental retardation disorders (Chen and Antonarakis, 1997; Chen et al., 1995; Guimera et al., 1996; Wittwer et al., 2001). However, it remains to be determined whether the human genes identified cause the respective disorders, and whether their functions have been conserved. In at least one case—fragile X syndrome—the gene responsible for the human disorder has been shown to have a single homolog in *Drosophila* (Wan et al., 2000), opening the door to the possibility of establishing a *Drosophila* model for a human mental retardation disorder.

Fragile X syndrome is the most common form of inherited mental retardation with an incidence of 1/3000–4000 males (Morton et al., 1997; Turner et al., 1996). The disease results from loss-of-function mutations in the *FMR1* gene at Xq27.3 (De Boulle et al., 1993; Pieretti et al., 1991; Gu et al., 1994; Lugenbeel et al., 1995; Meijer et al., 1994; Verkerk et al., 1991). Mental retardation and developmental delay are the most significant clinical features (Hagerman, 1996; O'Brien, 2000); however, other deficits, such as hyperactivity, autistic-like behavior, and macroorchidism are also associated with the disease (Hagerman, 1996).

The protein product of the *FMR1* gene, FMRP, contains multiple functional domains including three RNA binding domains, a nuclear export signal, and a nuclear localization signal (Eberhart et al., 1996; Siomi et al., 1993). It has been shown that FMRP can bind polyA RNA (Brown et al., 1998) and several candidate mRNA targets have recently been identified (Brown et al., 2001; Darnell et al., 2001). Consistent with fragile X pathology in patients, FMRP is highly expressed in the brain, especially in the hippocampus and the Purkinje cells of the cerebellum. FMRP expression is restricted to neurons and no expression has been detected in glia (Abitbol et al., 1993; Devys et al., 1993; Hergersberg et al., 1995; Tamanini et al., 1997). Autopsies of fragile X patients and studies of knockout mice have revealed defects in neurite density and morphology (Comery et al., 1997; Hinton et al., 1991; Irwin et al., 2000, 2001; Nimchinsky et al., 2001; Rudelli et al., 1985; Wisniewski et al., 1991), suggesting that *FMR1* may play a role in neurite branching. In addition, studies of transgenic mice overexpressing FMRP suggest that it functions in a dose-dependent manner (Peier et al., 2000).

Two highly related autosomal forms of *FMR1*, termed fragile X-related genes 1 and 2 (FXR1 and 2) have also been studied (Tamanini et al., 1997). Due to the similarity of the genes, it has been postulated that the autosomal forms can partially compensate for the loss of *FMR1*. This implies that the observed fragile X phenotype is milder than it might otherwise be and limits the utility of mouse models in understanding the function of *FMR1*. Therefore, other models would be useful for the analysis of *FMR1* function. An initial description of the fly *FMR1* homolog, *dfxr* (also called *dfmr1*), has been reported (Wan et al., 2000). The protein product, DFXR, is an RNA binding protein capable of interacting with itself and the mammalian counterparts, thus implying some degree of functional conservation. Expression studies indicate that DFXR is ubiquitously expressed and cytoplasmically localized. In addition, overexpression of DFXR in the eye and wing indicated that high doses of DFXR can cause cell death (Wan et al., 2000). More recently, a study of the *dfxr* phenotype reported that null mutations in the gene are viable and display peripheral (neuromuscular junction, NMJ) and central (optic lobe) synaptic

[5]Correspondence: bassem.hassan@med.kuleuven.ac.be

transmission defects (Zhang et al., 2001). These authors also reported a relatively modest increase in the number of arboreal branches at the NMJ and, probably consequently, a similar increase in the number of peripheral synaptic boutons. Neuronal overexpression of DFXR caused a decrease of bouton number, without affecting the number of branches. Finally, the authors present evidence that the upregulation of the *Drosophila* MAP1B homolog, Futsch, in *dfxr* mutants is sufficient to explain the defects observed in *dfxr* mutants, a surprising finding given the potentially large number of target RNAs of the mammalian FMRP protein.

To investigate *Drosophila* as a model for fragile X disease, we studied the loss and gain of DFXR function in the brain. First, we find that DFXR, like its mammalian homologs, is expressed in brain neurons but not in glia. Second, we show that in the brain, both loss and gain of DFXR function result in strong loss of neurite extension and irregular branching, as well as axon guidance defects in dorsal cluster (DC) neurons. Another cell type, the lateral neurons (LNv), shows variable defects in extension and guidance. Photoreceptor neurons, on the other hand, are morphologically normal. Consistently, all *dfxr* mutant alleles examined cause a failure in adult eclosion, and circadian rhythm defects, suggesting that the functions of the DC and LNv neurons are compromised; in contrast, synaptic transmission is apparently normal in photoreceptor neurons. These data argue that different neuronal subtypes are affected differentially by the loss of *dfxr*. Finally, we demonstrate that the severity of both the loss- and gain-of-function phenotypes depends on the level of DFXR activity, suggesting that DFXR acts in a dose-dependent manner to determine neuronal phenotype.

Results

DFXR Is Expressed in Brain Neurons but Not Glia

DFXR contains the same functional domains as its vertebrate homologs (Figure 1A) and is equally similar to all three forms, suggesting that it is derived from an ancestral protein (Figure 1B). We used four reported *dfxr* alleles (Zhang et al., 2001), one hypomorphic P element insertion allele and three null deletion alleles (Figure 1C), as well as *dfxr* transgenic flies (Wan et al., 2000) to study the effects of *dfxr* loss and gain of function. We began by examining the expression and distribution of DFXR in the fly brain. The mammalian FMR1 protein is enriched in the brain, but its expression is specific to neurons and excluded from glia. To determine the developmental regulation of DFXR brain expression, we analyzed pupal brains, immunohistochemically, at two stages of pupal development, as well as adult brains using α-DFXR, a neuronal specific marker (*elav* [c155] driven GFP) and glial specific (REPO) marker (Figure 2). We find that DFXR is constitutively expressed in most, if not all, neuronal cell bodies and excluded from glia (Figure 2A). This pattern persists in adults (Figure 2B). Importantly, no DFXR protein was detected in the brains of any *dfxr* deletion mutant we analyzed (Figure 2C).

dfxr Differentially Regulates Neurite Extension

In order to study the effect of *dfxr* loss in the CNS, the DC neurons were analyzed. These cells were chosen since they exhibit a simple stereotypical pattern of axon branching in the distal medulla, allowing any abnormalities to be readily observed (Hassan et al., 2000). In order to visualize these neurons in the mutant background, the DC marker *atoGal4-14A* construct was recombined onto the $dfxr^{\Delta 113}$ chromosome. In combination with *UAS-CD8gfp*, this recombinant chromosome allows the visualization of the DC neurons and their branching patterns. Flies were studied either as living pharate adults, or shortly after eclosion. First we established that DFXR is indeed expressed in DC neurons. We find that DFXR is present in DC neuronal cell bodies and localized to the cytoplasm during pupal development (data not shown), when DC neurons are arborizing in the optic lobes, as well as in adults (Figure 2D). The analysis of *atoGal4-14A,*$dfxr^{\Delta 113}$ flies, in various combinations with all the other mutant chromosomes, indicated that the number of cells and their relative positions are normal, suggesting that neurogenesis and cell division are normal. Two major defects were recorded in all *dfxr* mutants. First, by comparison to heterozygous siblings (Figure 3A), we observed a reduction in the number of DC neuron axons crossing from the lobula into the medulla (Figures 3B–3D). It should be noted that most axons that did cross toward the medulla seemed to do so at the correct positions, although others showed clear pathfinding defects (Figure 3B, arrow). The average number of crosses to the medulla ($\sim$3 crosses/brain lobe) was similar for all transheterozygous deletion allele combinations ($dfxr^{\Delta 50}$/$dfxr^{\Delta 113}$, $dfxr^{\Delta 83}$/$dfxr^{\Delta 113}$, and $dfxr^{\Delta 113}$/$dfxr^{\Delta 113}$). As expected, the hypomorphic $dfxr^{EP3517}$/$dfxr^{\Delta 113}$ combination showed a milder phenotype (average of 6 crosses/brain lobe) when compared to controls (Figure 3G).

We wondered whether DFXR is required for neurite extension in other neurons as is suggested by its pan-neuronal expression. To address this issue, we examined the morphology of the LNv, the major circadian rhythm centers in the fly brain (Helfrich-Forster et al., 2000). We confirmed that the LNv do indeed express the DFXR, and that it is cytoplasmically localized (Figure 3E, inset). In normal flies, LNv cells extend a dorsal branch toward the dorso-medial aspect of the brain. The branch first extends dorsally, and then turns medially toward the center of the brain at which point the individual fibers seem to defasciculate slightly. Labeling of the lateral neurons using UAS-CD8GFP driven by PDF-Gal4 (Renn et al., 1999) reveals two differences between heterozygous and homozygous mutant flies. First, by comparison to controls (Figure 3E), *dfxr* mutants (Figure 3F) show overextension of axons (red arrow), suggesting that in lateral neurons, *dfxr* normally inhibits neurite extension, whereas in DC neurons, it is required for proper extension. Another defect observed in lateral neurons is mistargeting of axons (yellow arrow) and looping of fibers (red arrowhead), suggesting potential guidance defects. In contrast to DC neurons, however, these defects showed considerable variation in severity among mutant animals. Severe defects shown in Figure 3F were observed in approximately 10% of mutant brains examined. Overall, approximately 40% of all brains examined showed phenotypes not observed in heterozygous siblings.

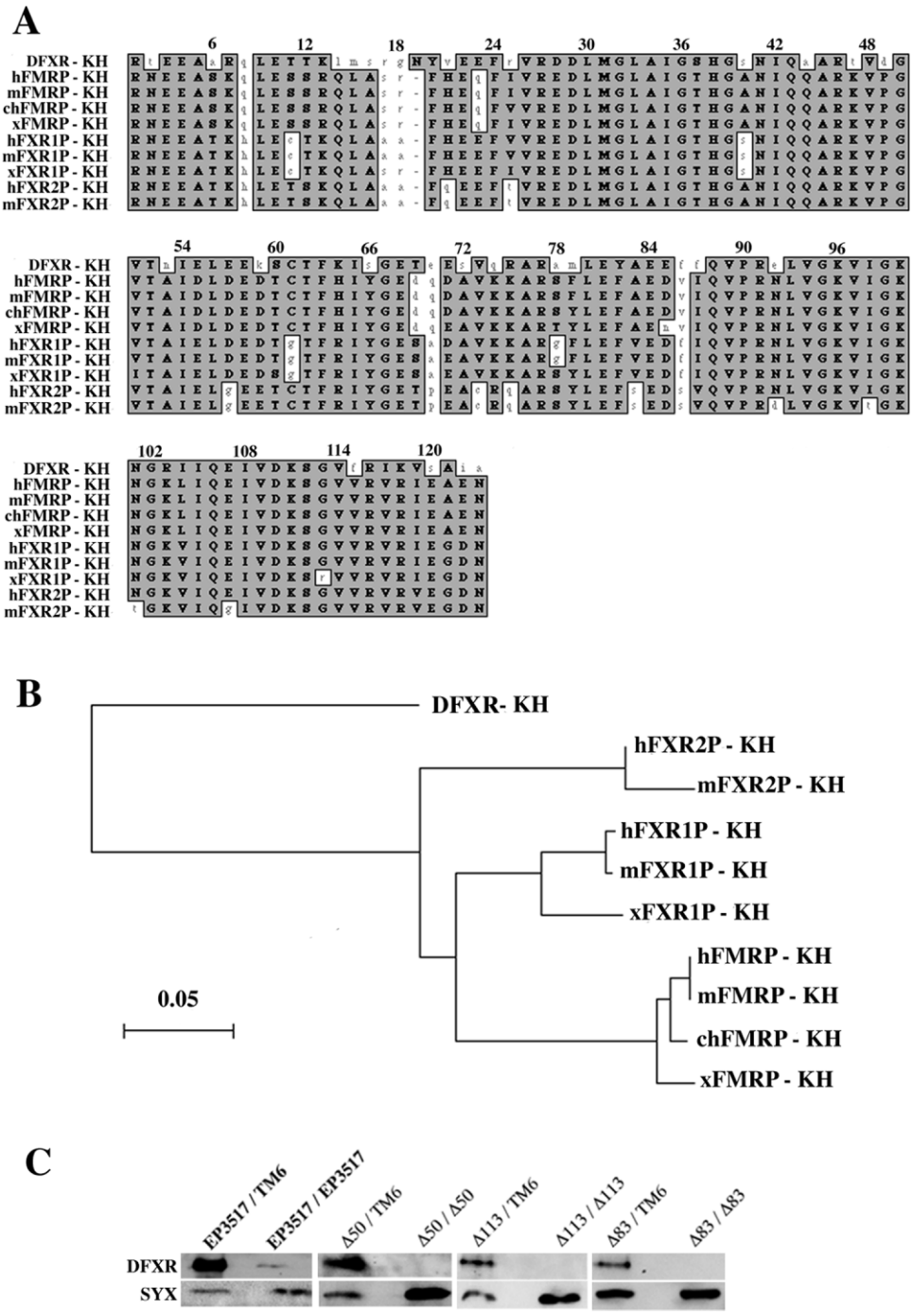

Figure 1. *dfxr* Is the Invertebrate Homolog of the Fragile X-Related Gene Family

(A) Amino acid sequence alignment of KH domains 1 and 2 of *Drosophila* DFXR; human and mouse FXR2P; human, mouse, and *Xenopus* FXR1P; and human, mouse, chicken, and *Xenopus* FMR1P. Identities and similarities are boxed and shaded. (B) Neighbor joining phylogenetic tree depicting the distance between pairs of sequences. The two most similar sequences were joined first. The other sequences were added one by one in order of decreasing similarity (MacVector Software). (C) Crude extracts were prepared from single mutant and heterozygous sibling flies and used for Western blot analysis. Monoclonal antibody 6A15 was used to immunodetect DFXR, and Syntaxin 1A (SYX) was used as a positive control. A reduced amount of DFXR in the $dfxr^{EP3517}$ line indicates that this mutant is a hypomorph. No DFXR protein was detected in any of the deletion lines in either adults or larvae (data not shown for larvae).

dfxr Mutants Display Eclosion and Circadian Rhythm Defects

The projection defects observed for the DC and LNv neurons in *DFXR* mutants suggested that there might be a perturbation of neuronal function. Defects affecting the DC neuronal population are known to cause eclosion failure (Hassan et al., 2000). Indeed, for several different *dfxr* alleles, we observed that homozygous mutants de-

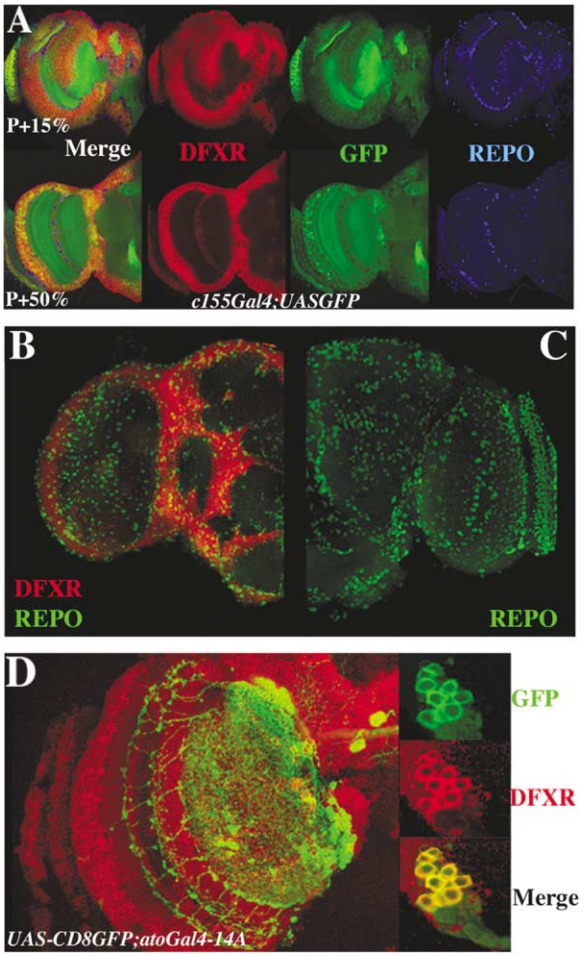

Figure 2. DFXR Is Expressed in Brain Neurons

(A) Pupal brains of c155Gal4; UAS-GFP animals, a neuronal marker (green), were stained at 15% (top; P + 15%) and 50% (bottom; P + 50%) of pupal development with α-DFXR (red) and α-REPO (blue), a glial marker. DFXR is highly expressed in the cell bodies of most, if not all, neurons but not in glia, during pupal development at a time when DC neuron axons are arborizing in the optic lobes. (B and C) Adult brains of wild-type (B) and *dfxr*$^{\Delta 113}$ deletion mutant (C) flies were stained with α-DFXR (red) and α-REPO (green). The neuronal specific expression persists in wild-type adult flies, whereas no DFXR expression is detected in mutant brains. No effects on glia or the gross organization of the brain are observed in mutants. (D) Adult brains of *UAS-GFP; atoGal4-14A* (green) flies were stained with α-DFXR (red). DFXR is highly expressed in DC neurons (left). Careful examination shows that DFXR is detectable in the cytoplasm, but not nuclei, of DC neurons (right).

velop until the pharate adult stage and then fail to eclose. It is important to point out that pupae from *TM6B* balanced mutant stocks, carrying the visible dominant *Tb* marker, were counted to insure that they had developed to the pharate adult stage in Mendelian ratios. Thus, the lethality quantified is due to eclosion failure and pharate adult lethality and not to lethality at earlier stages of development. This eclosion failure was further quantified by counting the number of eclosing adults for the different allelic strains (Table 1). Defective eclosion was most apparent for the *dfxr*$^{\Delta 50}$ and *dfxr*$^{\Delta 113}$ alleles, with fewer than 1% of adults emerging (Table 1). Mutants homozygous for the hypomorphic *dfxr*^{EP3517} insertion allele, which show milder morphological defects, also display a less severe eclosion phenotype. While this phenotype is reminiscent of flies with disrupted DC neurons, it should be noted that the observed eclosion phenotype may not be due to defects in DC neurons alone. Defects in other classes of fly neurons can also affect eclosion (Baker et al., 1999).

Effects on the lateral neurons, the circadian pacemaker cells of the fly brain (Ewer et al., 1992), are expected to perturb circadian clock output. As most of the *dfxr* alleles are semilethal, we were able to characterize adult behavior in "escaper" individuals. We examined circadian rhythms of locomotor activity in *dfxr*$^{\Delta 113}$ homozygous mutants and in sibling heterozygotes of similar genetic background. As shown in Figure 4A and Table 2, control heterozygous siblings had robust activity rhythms with an average circadian period in the wild-type range. In contrast, the vast majority of homozygous mutants exhibited weak and erratic rhythmicity or were statistically arrhythmic (Figures 4B and 4C). A few of the homozygotes (3/36; Table 2) showed a single dominant periodicity, by visual inspection of records and/or by X^2-periodogram analysis (i.e., they were considered strongly rhythmic), but the remainder of the rhythmic flies exhibited multiple free-running activity components in DD. These were noted by visual inspection of records and on the basis of X^2-periodogram analysis (Figure 4C). Compared to control siblings, homozygous *DFXR* mutants also displayed abnormally low average activity levels, although it is unclear how this phenotype relates to the circadian defect. Average daily activity levels in LD and DD, respectively, were 642 ± 313 (SD) and 539 ± 301 events for *dfxr* homozygotes, whereas they were 1533 ± 489 and 1891 ± 652 events for heterozygotes.

The alteration of locomotor activity rhythms in *dfxr* mutants could be due to an effect on the clock mechanism or, alternatively, a perturbation of a process downstream of the clock. To address this issue, we determined whether *dfxr* mutations also affected the circadian timing of adult eclosion, an independent rhythm controlled by the fly circadian clock system. Interestingly, eclosion exhibited normal circadian periodicity in DD; i.e., the medium of eclosion peaks was at ~CT12 on all 3 days of DD, indicating a normal 24 hr circadian period (Figure 5A). However, peaks of eclosion were phase delayed each day in the mutant by as much as 6–8 hr, relative to heterozygous (control) siblings (Figure 5B), and such a phenotype is consistent with an effect on rhythmicity that occurs downstream of the clock mechanism. Consistent with a downstream effect on rhythmicity, PERIOD (PER) protein exhibited normal circadian changes in abundance in both *dfxr* mutants and control heterozygotes (Figures 5C and 5D). This result, together with the observed rhythmic eclosion, indicates that the molecular oscillator is intact in *dfxr* mutants.

Normal Photoreceptor Morphology and Function in *dfxr* Mutants

The effects of *dfxr* mutations on DC and LNv neurons suggested that DFXR might regulate morphology and/or function differently in distinct neuronal populations, perhaps depending on which RNA targets are regulated by the protein in the different neurons. To investigate DFXR function in another class of neurons, we per-

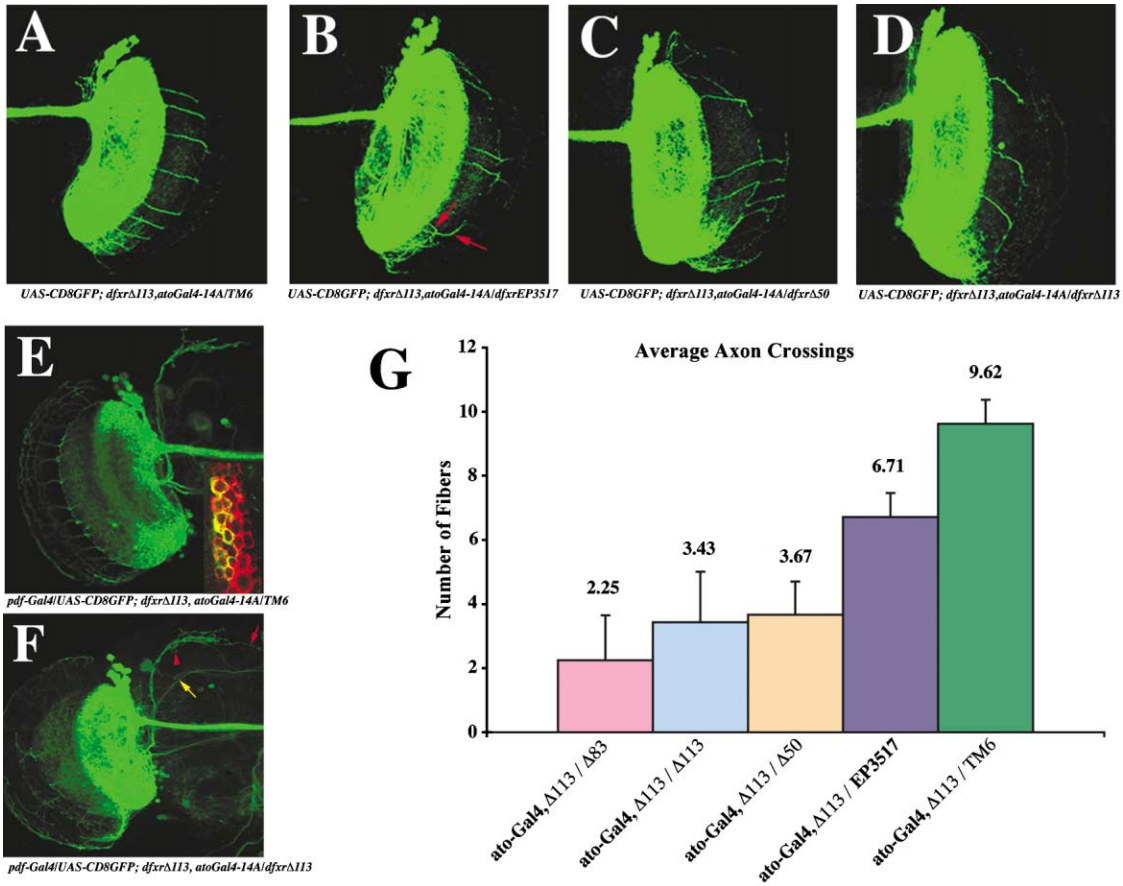

Figure 3. Mutant Flies Exhibit a Fiber Extension Defect in the DC and LNv

Brains of homozygous mutant flies and their heterozygous siblings expressing GFP specifically in DC neurons or LNv were stained with α-GFP. (A) Confocal section through a *UAS-CD8GFP; atoGal4-14A,dfxr$^{\Delta 113}$/TM6* adult brain. Normal axon extension from the lobula to the medulla was observed. (B) Confocal section through a *UAS-CD8GFP; atoGal4-14A,dfxr$^{\Delta 113}$/dfxr^{EP3517}* adult brain. A reduction in the number of fibers is observed. Some fibers show guidance defects (arrows). (C and D) Confocal sections through null mutant adult brains stained for GFP: (C) *UAS-CD8GFP; atoGal4-14A,dfxr$^{\Delta 113}$/dfxr$^{\Delta 50}$*, (D) *UAS-CD8GFP; atoGal4-14A,dfxr$^{\Delta 113}$/dfxr$^{\Delta 113}$*. All null mutants show a similar reduction in the number of fibers crossing the optic chiasm between the lobula and medulla. (E) Confocal section through a *UAS-CD8GFP/PDF-Gal4; atoGal4-14A,dfxr$^{\Delta 113}$/TM6* adult brain showing the normal pattern of dorsal branch extension of LNv. Inset shows a magnification of confocal section through a *UAS-CD8GFP/PDF-Gal4* adult brain stained for GFP (green) and DFXR (red) showing colocalization (yellow) of DFXR with GFP and its expression in the cell bodies of LNv cells (arrowheads). (F) Confocal section through a *UAS-CD8GFP/PDF-Gal4; atoGal4-14A,dfxr$^{\Delta 113}$/dfxr$^{\Delta 113}$* adult brain showing two defects in axon extension. First, some fibers extend significantly further than others (red arrow). Second, other fibers display what appear to be guidance defects taking either a completely different route (yellow arrow) or displaying aberrant morphology (red arrowhead). The staining and phenotype of the DC neurons were used as an additional confirmation of the genotype of the brains. (G) Quantification of the fiber extension phenotype. A total of ten half brains were evaluated for each genotype and fibers were counted from each and the average calculated. Error bars of the deletion mutant samples overlap suggesting that the differences among the null mutants are not significant.

formed electroretinogram (ERG) recordings for homozygous mutants and control heterozygotes to examine photoreceptor synaptic transmission (Figures 6A and 6B). We also examined the structure of photoreceptor axons and terminals in the optic lobes using α-chaoptin (mAb 24B10; Figure 6C). These studies demonstrated that photoreceptor development and function are not affected by loss of DFXR. We find that the "on" (Figure 6A-1) and "off" (Figure 6A-2) transients of ERGs are not significantly different between *dfxr* homozygotes and control flies of similar genetic background (*w*). This was surprising since it had been reported that *dfxr* mutants show a decrease in the amplitude of the off transient (Zhang et al., 2001). A possible reason for this discrepancy is that wild-type flies, rather than genetic background controls, were used by Zhang et al. To test this idea, we recorded ERGs from wild-type Canton S (*CS*) flies. Indeed, we also found that *CS* flies have a larger off transient than either *w* control or *dfxr* mutant flies (Figure 6A-2). These observations indicate that *dfxr* mutations do not affect the ERG, and emphasize the importance of proper genetic controls in physiological and behavioral studies. The examination of photoreceptor axons in the lamina (la), optic chiasm (oc), and distal medulla (dm) indicates that guidance, targeting, and terminal field morphology are normal in the *dfxr* mutant (Figure 6C).

dfxr Regulates Neurite Branching

In addition to neurite extension defects, *dfxr* mutants exhibit aberrant neurite branching patterns. In wild-type animals, fibers of the DC neurons enter the medulla and

Table 1. Quantification of Eclosion Defects in Homozygous *dfxr* Mutants

Genotype	Obs. # of Eclosed Flies	Exp. # of Eclosed Flies[a]	% of Obs/Exp. Eclosed Flies[a]
$dfxr^{EP3517}/TM6$	130	116	112%
$dfxr^{\Delta 50}/TM6$	117	78	150%
$dfxr^{\Delta 83}/TM6$	115	88	130%
$dfxr^{\Delta 113}/TM6$	1038	694	150%
$dfxr^{EP3517}/dfxr^{EP3517}$	44	58	79.5%
$dfxr^{\Delta 50}/dfxr^{\Delta 50}$	0	39	0%
$dfxr^{\Delta 83}/dfxr^{\Delta 83}$	16	44	36.4%
$dfxr^{\Delta 113}/dfxr^{\Delta 113}$	3	347	0.86%

Based on at least three vials for each genotype; for each allele, heterozygotes and homozygotes eclosed from the same vials.
[a] #, and therefore %, of expected flies is based on the assumption of 100% viability for homozygous mutants.

then branch in a regular array, forming a stereotypical grid-like structure shown in Figure 7A for heterozygous *dfxr* flies. In contrast, transheterozygous flies bearing several different *dfxr* allelic combinations ($dfxr^{\Delta 50}/dfxr^{\Delta 113}$, $dfxr^{\Delta 83}/dfxr^{\Delta 113}$, and $dfxr^{\Delta 113}/dfxr^{\Delta 113}$) exhibited defects in the formation of this structure. In the mutants, small ectopic branches were observed (Figures 7B and 7C), suggesting a misregulation of the intrinsic branching program. It could also be the case, however, that aberrant branching is a consequence of a reduced number of fibers entering the medulla. Perhaps the formation of the grid-like neurite branches is dependent on the presence of several neighboring fibers, rather than being regulated autonomously in each fiber. To test this possi-

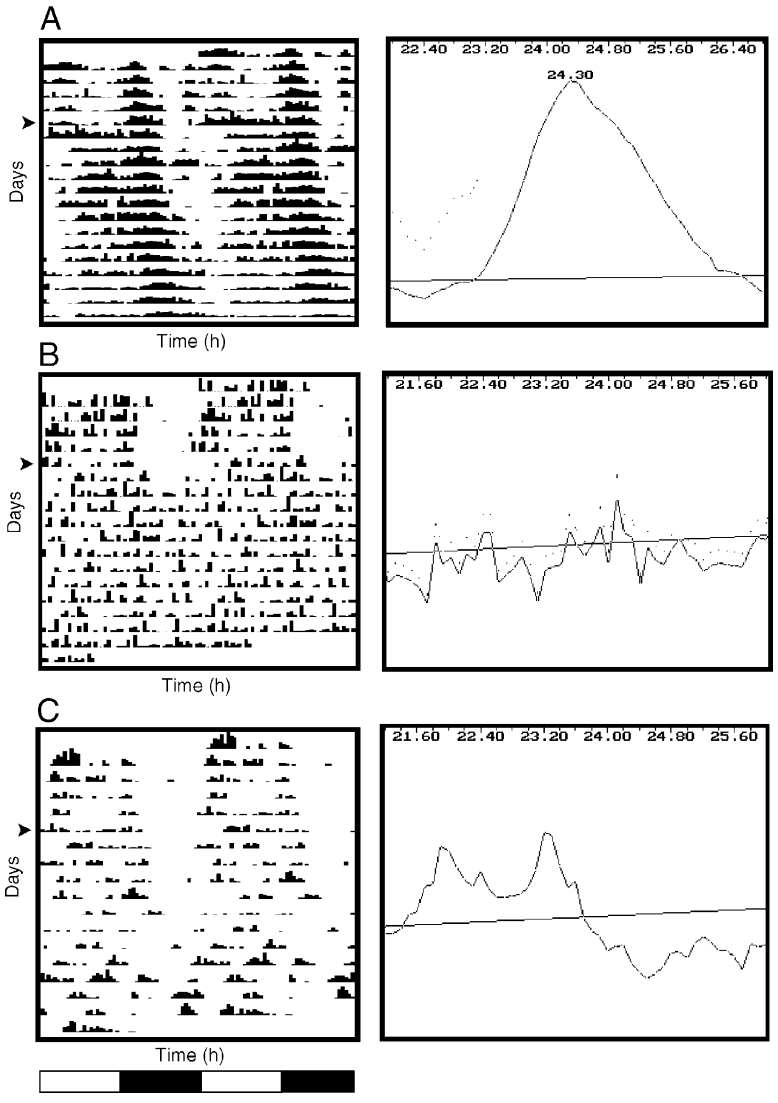

Figure 4. *dfxr* Mutants Display Locomotor Activity Rhythm Defects

Records of locomotor activity from two DFXR homozygotes (B and C) and from a control heterozygote (A). Activity records are double plotted, with the first day of activity at the top and subsequent days plotted beneath. Periodogram plots are shown to the right of each locomotor activity record. Black histograms represent bouts of activity. Arrowheads adjacent to the Y axes indicate the day on which individuals were transferred to constant darkness (DD). Flies were entrained to a light:dark cycle consisting of 12 hr of light and 12 hr of dark (LD12:12) for 4–5 days, and then transferred to DD for about 2 weeks. The open and dark rectangles at the bottom of the figure indicate the LD cycle during entrainment.

Table 2. Summary of Circadian Parameters for DFXR Heterozygotes and Homozygotes

Genotype	n	# Arrhythmic	# Strongly Rhythmic[a]	# Weakly Rhythmic[a]	% Strongly Rhythmic	% Weakly Rhythmic	$\tau \pm$ SEM[b]
DFXR/+	65	5	60	0	92.3	0	23.6 ± 0.01
DFXR/DFXR	36	25	3	8	8.3	22.2	24.1 ± 0.20

[a] Strong and weak rhythmicity were quantitated using the rhythmicity index (RI) described in Experimental Procedures.
[b] Calculated using the strongly and weakly rhythmic flies.

bility, we examined the branching pattern in the *dfxr*^{EP3517}/*dfxr*$^{\Delta 113}$ combination, for which more than 60% of fibers cross to the medulla (Figure 3G). Flies bearing this allelic combination also showed defects in the branching pattern and small ectopic branches (Figure 7D), despite the presence of several neighboring fibers that extended in a regular array. These data indicate that the branching defect is not secondary to the crossing defect.

DFXR Functions in a Dose-Dependent Manner

We were interested to determine whether, and how, gain of DFXR function might also affect neurite morphology. Therefore, we examined the effect of *dfxr* overexpression on DC neuronal morphology. We found that high levels of DFXR caused a complete failure of axon extension from the lobula to the medulla (Figure 7E) in every brain examined. This is qualitatively very similar to the loss-of-function mutant phenotype, but more severe. Careful analysis of flies overexpressing DFXR showed that fibers entered the lobula (Figure 7E, arrows), but that they then projected to inappropriate sites within the lobula or stopped at the lobula-medulla border (Figure 7E, arrowheads). To confirm that this phenotype was dependent on the level of DFXR activity, we overexpressed a mutant form of the protein. This mutant protein carries a missense mutation (I307N) in a highly conserved Isoleucine of the KH domain, mimicking a mutation identified in a severe case of fragile X syn-

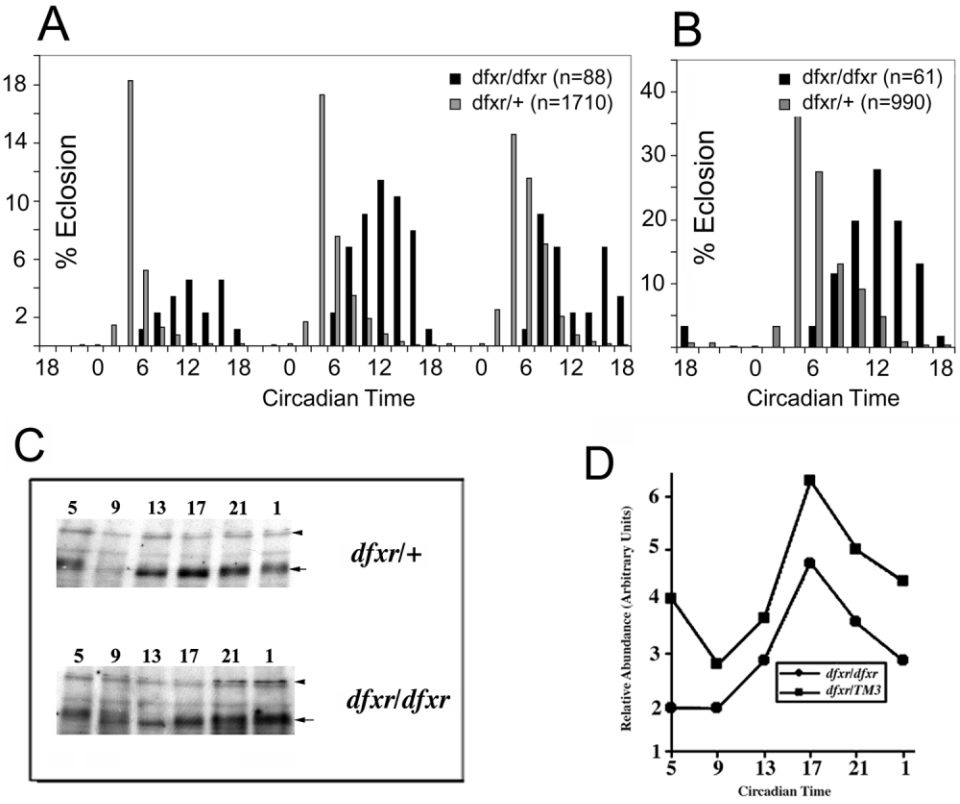

Figure 5. Rhythms of Adult Eclosion and PER Cycling in *dfxr*/*dfxr* and *dfxr*/+ Populations

(A) Plot of 3 days of continuous eclosion behavior for the two types of populations. This experiment was carried out twice with similar results. (B) Pooled data from day 2 of constant darkness (DD) for two independent eclosion experiments. In both panels, data (eclosed flies) are normalized by plotting the flies that eclosed in any given 2 hr bin as a percent of the total number of flies in the experiment. The number of flies in the different populations is indicated in parentheses beside each genotype. Circadian time is the time in DD. (C) Circadian increases in PER protein abundance (arrow) in *dfxr*/*dfxr* and *dfxr*/+ flies during day 2 of DD. Numbers at the top of the two panels refer to circadian time. Note that lane 5 of the *dfxr*/*dfxr* gel contained about half the amount of protein as other lanes. Arrowheads refer to a nonspecific band detected by the PER antibody whose levels were used to normalize PER protein abundance. (D) Relative abundance of PER protein in *dfxr*/*dfxr* and *dfxr*/+ flies, expressed as a ratio of PER to a nonspecific band seen with the PER antiserum.

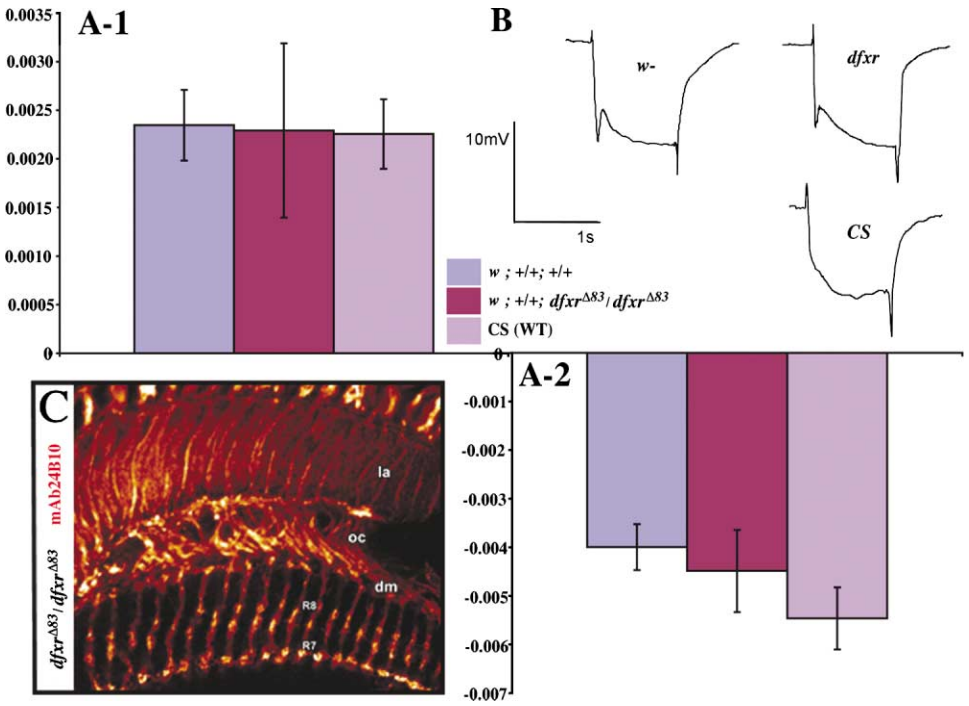

Figure 6. Photoreceptor Neurons Are Normal

(A) Average size of the "on" and "off" (A2) transient amplitudes. No significant differences are detected between wild-type (*CS*), genetic controls (*w*), and *dfxr* mutants in the "on" transient (A-1). The "off" transient shows no statistically significant difference between *w* and *dfxr* mutants; however, mutants show a decrease relative to *CS* (A-2). (B) Sample ERG traces for *CS*, *w*, and *dfxr* mutant flies. (C) mAb 24B10 (α-chaoptin) of photoreceptor field in the optic lobes (Lamina [la], optic chiasm [oc], distal medulla [dm]) of *dfxr* mutant flies. No defects are detectable.

drome (De Boulle et al., 1993). Wan et al. (2000) had shown that this form of the protein has reduced activity by comparison to the wild-type protein. Indeed, overexpression of DFXR^{I307N} resulted in defects similar to but less severe than those seen in loss-of-function mutants (Figures 7F and 7G). In overexpressing individuals, only occasionally were fibers observed to cross the lobula-medulla border. However, those fibers formed aberrant projection and branching patterns within the medulla (Figure 7G, arrows), consistent with a role for DFXR in both processes. We also expressed DFXR in the DC neurons of *dfxr* mutants (*UAS-dfxr/UAS-CD8gfp; dfxr$^{\Delta 83}$/dfxr$^{\Delta 113}$, atoGal4-14A* and *UAS-dfxr/UAS-CD8gfp; dfxr$^{\Delta 113}$/dfxr$^{\Delta 113}$, atoGal4-14A*). We find that expression of *dfxr* in the absence of any detectable endogenous protein has the same effect as expression in a wild-type background (Figure 7H). These data suggest that the dose of DFXR may be under stringent regulation and that precise levels are required for proper function.

Discussion

dfxr Regulates Neurite Morphology

To investigate the function of the *Drosophila* fragile X homolog, *dfxr*, and investigate *Drosophila* as a model for fragile X syndrome, we studied the effect of the loss and gain of function of *dfxr* in the fly brain. DFXR displays two important similarities to the human protein. First, it has significant sequence similarity in the functional domains. Second, while it is widely and dynamically expressed, in the brain its expression is restricted to neurons and excluded from glia. Considering that the most significant phenotype of fragile X patients is mental retardation and that the mammalian gene has been implicated in the regulation of neurite morphology, it was of significant interest to show that this model could be used to study neuronal phenotypes in the *Drosophila* brain. Analysis of DC and LNv cells in *dfxr* mutants shows that the loss of DFXR causes axon extension defects. In DC neurons, all mutant brains examined showed failure of axon extension. Importantly, this extension defect was less severe in hypomorphic mutants expressing low levels of the protein; i.e., the level of DFXR activity is proportional to the observed phenotype. In contrast, overextended axons were observed for LNv neurons, indicating that DFXR acts to inhibit axon extension in these cells. Interestingly, not all *dfxr* mutant brains exhibited LNv neuronal defects, suggesting that the role of DFXR may be redundant in these cells. Finally, photoreceptor neurons appear morphologically normal in mutants, demonstrating that DFXR activity is differentially required within the nervous system. Interestingly, overexpression of DFXR in DC neurons, both in wild-type and mutant backgrounds, resulted in a complete failure of axon extension. Therefore, loss and gain of function lead to similar phenotypic defects, potentially suggesting that the dosage of DFXR is critical for its function. In vertebrates, it has been shown that the dosage of the protein was correlated with behavioral abnormalities (Peier et al., 2000). In addi-

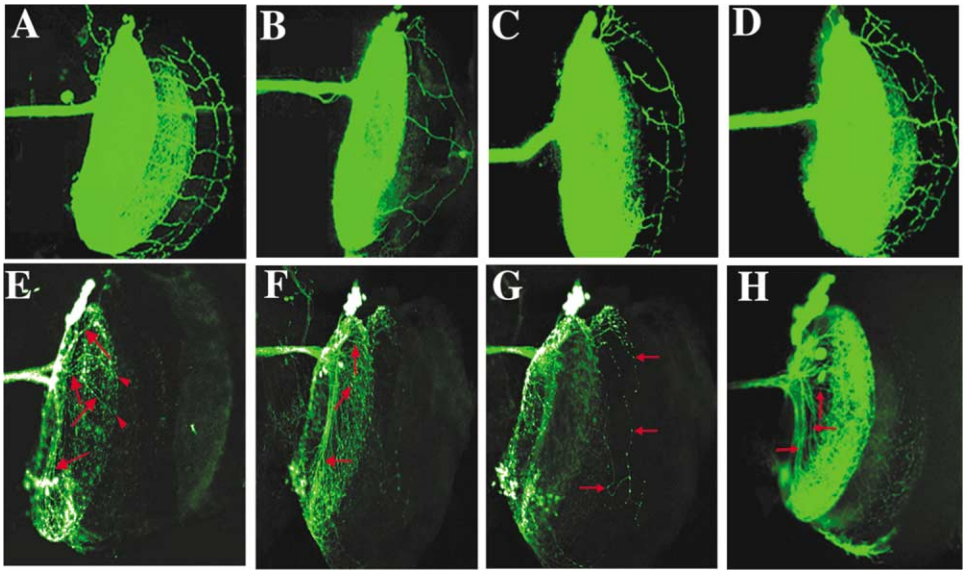

Figure 7. *dfxr* Regulates Neurite Extension and Branching in a Dose-Dependent Manner

Brains of homozygous mutant flies and their heterozygous siblings expressing GFP specifically in DC neurons were stained with α-GFP. (A) Confocal section through a *UAS-CD8GFP; atoGal4-14A,dfxr$^{\Delta 113}$/TM6* adult brain stained for GFP. The stereotypical grid-like structure in the distal medulla is readily distinguishable. (B–D) Confocal sections through mutant adult brains stained for GFP. The few axons which extended toward the distal medulla in the null mutants *UAS-CD8GFP; atoGal4-14A,dfxr$^{\Delta 113}$/dfxr$^{\Delta 50}$* (B) and *UAS-CD8GFP; atoGal4-14A,dfxr$^{\Delta 113}$/dfxr$^{\Delta 113}$* (C) show severe defects in their branching patterns forming short thin branches that fail to connect. (D) Confocal section through a *UAS-CD8GFP; atoGal4-14A,dfxr$^{\Delta 113}$/dfxr^{EP3517}* adult brain showing severe defects in neurite branching despite a significant number of neighboring axons having crossed toward the distal medulla. (E) Confocal section through a *UAS-dfxr/+; UAS-LacZ, atoGal4-14A/+* adult brain stained with α-βGal. Overexpression of DFXR in the DC cells of wild-type flies causes a complete failure of axons to cross from the lobula to the medulla. Arrows indicate axons that projected to inappropriate sites and arrowheads axons that stopped at the lobula-medulla border. (F and G) Confocal sections through *UAS-dfxr^{I307N}/+; UAS-LacZ, atoGal4-14A/+* adult brains stained with α-βGal. Overexpression of hypomorphic DFXR^{I307N} protein results in a similar, but less severe, phenotype. Most axons either project inappropriately in the lobula (arrows) or stop at the lobula/medulla border (F). Some axons cross toward the distal medulla but display guidance (arrows) and branching (arrowheads) defects (G). (H) Confocal sections through *UAS-CD8GFP/UAS-dfxr; dfxr$^{\Delta 113}$, atoGal4-14A/dfxr$^{\Delta 83}$* adult brains stained for GFP. Expression of *dfxr* in the absence of any detectable endogenous protein has the same effect as expression in a wild-type background. Arrows indicate axons that projected to inappropriate sites within the lobula.

tion to neurite extension defects, neurite branching abnormalities were observed for the DC neurons in *dfxr* mutants. It is important to note that even hypomorphic allelic combinations showed strong branching defects. This suggests that DFXR regulates extension and branching independently, and this can be most easily explained by assuming that each process requires a different set of DFXR targets.

dfxr Mutants Display Behavioral Defects

In addition to neuronal morphology, we studied the role of DFXR in neuronal function. Several defects were observed. First, large numbers of *dfxr* mutants fail to eclose and die as fully developed pharate adults with no visible morphological defects. This phenotype may be the consequence of an underlying neural defect since DFXR is expressed within the DC neurons, and a similar eclosion phenotype is observed with lesions affecting the DC neurons. However, as DFXR is expressed in many different neurons, defective eclosion may arise from a perturbation of another cell type.

dfxr mutants also exhibit abnormal circadian behavior, although the characterization of eclosion rhythms and PER cycling in mutant populations indicates that the molecular clock is intact. The alteration of circadian behavior may arise as a consequence of defects in the LN_v neuronal projections or because of functional changes within the LN_v population. While the LN_v morphological phenotypes were variable in severity and observed in fewer than half the mutants, circadian locomotor activity defects were seen in most mutant flies. One possibility is that some individuals have subtle synaptic morphology defects (Zhang et al., 2001) that are nonetheless severe enough to impair LNv function. Alternatively, it may be that loss of DFXR impairs a different aspect of LNv function such as the rhythmic release of the PDF neuropeptide, which is known to be critical for the circadian regulation of behavior (Helfrich-Forster et al., 2000; Park et al., 2000). Interestingly, it has been reported that fragile X patients exhibit increased variability in total sleep time and problems with sleep maintenance (Gould et al., 2000), phenotypes that might be due to abnormal circadian regulation.

DFXR Has Differential Actions

Observations on DFXR function in the central brain, NMJ, and the retina/optic lobe complex indicate that the protein not only regulates multiple processes within a class of neurons, but also regulates these processes differentially between different classes of neurons. Mechanistically, this can be best explained by assuming that the phenotypically relevant targets of DFXR regula-

tion are (1) diverse and (2) vary from one cell type to another. Thus, while the rescue of DFXR phenotypes by MAP1B mutants suggests that upregulation of MAP1B in the absence of DFXR may be sufficient to explain the peripheral phenotypes, it is very difficult to imagine how it would suffice to explain the diverse, variable, and contrasting central defects. That is, a perturbation of other targets must be the cause of the central defects. Examples include the RhoGAP P190, which is known to be required for neurite extension and has been implicated in mental retardation (Billuart et al., 1998, 2001; Brouns et al., 2000, 2001; Kutsche et al., 2000), and the Semaphorins, which are regulators of growth cone guidance (Van Vactor and Lorenz, 1999). The description of neuronal phenotypes in *Drosophila dfxr* mutants will permit genetic studies to identify potential targets and other components of the signaling pathways that are relevant for an understanding of fragile X pathogenesis.

Experimental Procedures

Fly Strains and Genetics

dfxr mutant lines, the EP parental line, and *w;UAS-dfxr* lines were obtained from A. Bailey and G. Rubin at the University of California, Berkeley and are described in Zhang et al. (2001). The deficiency line *Df(3R)by62* was obtained from the Bloomington Stock Center. *y,w; UAS-CD8gfp* and *y,w,elavGal4-c155,UASCD8gfp* were obtained from Liqun Luo and are described in Lee and Luo (1999). *y,w;;atoGal4-14A* is described in Hassan et al. (2000). All stocks were raised on standard fly food and the crosses were performed at 25°C. The Tb^+ and *Hu* markers on the *TM6B* balancer chromosome were used to distinguish mutant animals from their heterozygous siblings. In addition, the *L* marker and *CyO* chromosome were used to follow the segregation of *UAS-dfxr* and *UAS-CD8gfp* transgenes.

Expression Analysis

For protein analysis, total protein was extracted from single larvae or adults by pressing in Standard Loading Dye (SDS, bromophenol blue, DTT, glycerol, and *B* mercaptoethanol) followed by incubation at 98°C for 10 min. The crude extract was separated by SDS-PAGE in a 10% mini gel (Bio-Rad Mini-Protean II Cell system) and electroblotted onto PVDF membranes (NEN). Monoclonal antibody 6A15 (courtesy of G. Dreyfuss) was used to immunodetect DFXR and an antibody against Syntaxin 1A (1C8) was used as an internal control for protein loading. The appropriate secondary antibodies were coupled to horseradish peroxidase and detected by the chemiluminescence method (ECL KIT, Amersham, Arlington Heights, IL). Immunohistochemistry was performed as described (Hassan et al., 2000). Briefly, adult brains were dissected from heads in PBS (phosphate buffered saline) and fixed with 4% formaldehyde in 1 × PBT (1 × PBS + 0.3% Triton X-100) for 20 min. Fixed brains were incubated overnight in 1 × PAXDG Buffer (PBT, 5% normal goat serum, 1% bovine serum albumin, 0.1% deoxycholate, and 1% Triton X-100) with either anti-DFXR (6A15, 1:1000) or anti-GFP (1:500). This incubation was followed by several washes in PBT (1 hr) and a final incubation with the appropriate secondary antibodies (1:250, 2 hr). Visualization was by confocal microscopy (BioRad 1024).

Behavioral Analysis

Locomotor activity was monitored in single flies using monitors from Trikinetics as described in previous studies (Levine et al., 1994). Activity records were visualized using the program Tau (Mini-Mitter, Inc.) and analyzed for circadian periodicity using a χ^2-periodogram program that is a component of the Tau package. Individuals were considered rhythmic if there was evidence of periodicity by visual inspection of records and clear peaks in the periodogram. Strongly rhythmic individuals were distinguished from weakly rhythmic flies using the rhythmicity index (RI) of Levine et al. (2002). The RI is a numerical description of the strength of a rhythm, which is obtained from the third peak of a rhythmic correlogram (the first peak occurs at lag 0). The value at this peak has been used to describe rhythm strength in studies on *Drosophila* heart and on molecular circadian rhythms (see Levine et al., 2002 for details of the method). Flies having a threshold value greater than 0.2 were classified as strongly rhythmic. Eclosion rhythms were monitored in constant darkness (DD) according to methods described in Newby et al. (1991). Briefly, developing cultures were maintained in a 12:12 light:dark cycle at 18°C for approximately 14 days. Cultures were then transferred to DD, and newly emerged adults were collected at 2 hr intervals for 1 to 3 days. To assess PERIOD protein cycling, adult male flies were entrained to LD 12:12 for 4 days and then transferred to constant darkness. Twenty hours after the final lights off, groups of flies were collected at 4 hr intervals throughout the circadian cycle to generate protein extracts. For each time point, extracts were prepared from a sample of 20 fly heads. Standard denaturing gels were prepared for protein blots, with each gel lane containing 40 ug head protein. A guinea pig anti-PER antibody (Lee et al., 1998) was employed at a dilution of 1/3000 to assess PER abundance at different times of day.

Electrophysiology

Wild-type (Canton S), *white*, and $dfxr^{\Delta 83}/dfxr^{\Delta 83}$ mutant flies were immobilized on coverslips in nail polish. ERG recordings were performed as described (Heisenberg, 1971) using glass electrodes. The light stimuli originated from an unfiltered white lamp and recordings were performed on dark-adapted flies for a period of 1 s. The reading was repeated once and the on and off transients measured and averaged.

Acknowledgments

We thank Mary Roberts for invaluable technical assistance in behavioral studies, Michael Greenbaum for help with ERG studies, and Joel Levine and Jeff Hall for help with determining the "strength" of locomotor activity rhythms. We thank Adina Bailey and Gerald Rubin for providing *dfxr Drosophila* lines that made this study possible, as well as Gideon Dreyfuss for providing α-DFXR antibody (mAb6A15) and Isaac Edery for α-PER antibodies. We also thank Hugo Bellen, Bart De Strooper, and Wim Annaert for comments on the manuscript. Funding from NIH R01 grants HL59873 (to F.R.J.) and HD29256 (to D.L.N.) contributed to this work. B.H. was funded by an NRSA postdoctoral fellowship during the initial parts of this project, and by the VIB for the later parts.

Received: December 26, 2001
Revised: April 10, 2002

References

Abitbol, M., Menini, C., Delezoide, A.L., Rhyner, T., Vekemans, M., and Mallet, J. (1993). Nucleus basalis magnocellularis and hippocampus are the major sites of FMR-1 expression in the human fetal brain. Nat. Genet. *4*, 147–153.

Baker, J.D., McNabb, S.L., and Truman, J.W. (1999). Hormonal coordination of behavior and physiology at adult ecdysis in *Drosophila melanogaster*. J. Exp. Biol. *202*, 3037–3048.

Billuart, P., Bienvenu, T., Ronce, N., des Portes, V., Vinet, M.C., Zemni, R., Carrie, A., Beldjord, C., Kahn, A., Moraine, C., and Chelly, J. (1998). Oligophrenin 1 encodes a rho-GAP protein involved in X-linked mental retardation. Pathol. Biol. *46*, 678.

Billuart, P., Winter, C.G., Maresh, A., Zhao, X., and Luo, L. (2001). Regulating axon branch stability. The role of p190 RhoGAP in repressing a retraction signaling pathway. Cell *107*, 195–207.

Brouns, M.R., Matheson, S.F., Hu, K.Q., Delalle, I., Caviness, V.S., Silver, J., Bronson, R.T., and Settleman, J. (2000). The adhesion signaling molecule p190 RhoGAP is required for morphogenetic processes in neural development. Development *127*, 4891–4903.

Brouns, M.R., Matheson, S.F., and Settleman, J. (2001). p190 RhoGAP is the principal Src substrate in brain and regulates axon outgrowth, guidance and fasciculation. Nat. Cell Biol. *3*, 361–367.

Brown, V., Small, K., Lakkis, L., Feng, Y., Gunter, C., Wilkinson,

K.D., and Warren, S.T. (1998). Purified recombinant Fmrp exhibits selective RNA binding as an intrinsic property of the fragile X mental retardation protein. J. Biol. Chem. *273*, 15521–15527.

Brown, V., Jin, P., Ceman, S., Darnell, J.C., O'Donnell, W.T., Tenenbaum, S.A., Jin, X., Feng, Y., Wilkinson, K.D., Keene, J.D., et al. (2001). Microarray identification of FMRP-associated brain mRNAs and altered mRNA translational profiles in fragile X syndrome. Cell *107*, 477–487.

Chen, H., and Antonarakis, S.E. (1997). Localisation of a human homologue of the Drosophila mnb and rat Dyrk genes to chromosome 21q22.2. Hum. Genet. *99*, 262–265.

Chen, K.S., Gunaratne, P.H., Hoheisel, J.D., Young, I.G., Miklos, G.L., Greenberg, F., Shaffer, L.G., Campbell, H.D., and Lupski, J.R. (1995). The human homologue of the Drosophila melanogaster flightless-I gene (flil) maps within the Smith-Magenis microdeletion critical region in 17p11.2. Am. J. Hum. Genet. *56*, 175–182.

Comery, T.A., Harris, J.B., Willems, P.J., Oostra, B.A., Irwin, S.A., Weiler, I.J., and Greenough, W.T. (1997). Abnormal dendritic spines in fragile X knockout mice: maturation and pruning deficits. Proc. Natl. Acad. Sci. USA *94*, 5401–5404.

Darnell, J.C., Jensen, K.B., Jin, P., Brown, V., Warren, S.T., and Darnell, R.B. (2001). Fragile X mental retardation protein targets G quartet mRNAs important for neuronal function. Cell *107*, 489–499.

De Boulle, K., Verkerk, A.J., Reyniers, E., Vits, L., Hendrickx, J., Van Roy, B., Van den Bos, F., de Graaff, E., Oostra, B.A., and Willems, P.J. (1993). A point mutation in the FMR-1 gene associated with fragile X mental retardation. Nat. Genet. *3*, 31–35.

Devys, D., Lutz, Y., Rouyer, N., Bellocq, J.P., and Mandel, J.L. (1993). The FMR-1 protein is cytoplasmic, most abundant in neurons and appears normal in carriers of a fragile X premutation. Nat. Genet. *4*, 335–340.

Eberhart, D.E., Malter, H.E., Feng, Y., and Warren, S.T. (1996). The fragile X mental retardation protein is a ribonucleoprotein containing both nuclear localization and nuclear export signals. Hum. Mol. Genet. *5*, 1083–1091.

Ewer, J., Frisch, B., Hamblen-Coyle, M.J., Rosbash, M., and Hall, J.C. (1992). Expression of the period clock gene within different cell types in the brain of Drosophila adults and mosaic analysis of these cells' influence on circadian behavioral rhythms. J. Neurosci. *9*, 3321–3349.

Gould, E.L., Loesch, D.Z., Martin, M.J., Hagerman, R.J., Armstrong, S.M., and Huggins, R.M. (2000). Melatonin profiles and sleep characteristics in boys with fragile X syndrome: a preliminary study. Am. J. Med. Genet. *95*, 307–315.

Gu, Y., Lugenbeel, K.A., Vockley, J.G., Grody, W.W., and Nelson, D.L. (1994). A de novo deletion in FMR1 in a patient with developmental delay. Hum. Mol. Genet. *3*, 1705–1706.

Guimera, J., Casas, C., Pucharcos, C., Solans, A., Domenech, A., Planas, A.M., Ashley, J., Lovett, M., Estivill, X., and Pritchard, M.A. (1996). A human homologue of Drosophila minibrain (MNB) is expressed in the neuronal regions affected in Down syndrome and maps to the critical region. Hum. Mol. Genet. *5*, 1305–1310.

Hagerman, R.J. and Cronister, A. (1996). Fragile X Syndrome: Diagnosis, Treatment and Research, 2nd Edition (Baltimore, MD: Johns Hopkins University Press).

Hassan, B.A., Bermingham, N.A., He, Y., Sun, Y., Jan, Y.N., Zoghbi, H.Y., and Bellen, H.J. (2000). *atonal* regulates neurite arborization but does not act as a proneural gene in the *Drosophila* brain. Neuron *25*, 549–561.

Heisenberg, M. (1971). Separation of receptor and lamina potentials in the electroretinogram of normal and mutant Drosophila. J. Exp. Biol. *55*, 85–100.

Helfrich-Forster, C., Tauber, M., Park, J.H., Muhlig-Versen, M., Schneuwly, S., and Hofbauer, A. (2000). Ectopic expression of the neuropeptide pigment-dispersing factor alters behavioral rhythms in Drosophila melanogaster. J. Neurosci. *20*, 3339–3353.

Hergersberg, M., Matsuo, K., Gassmann, M., Schaffner, W., Luscher, B., Rulicke, T., and Aguzzi, A. (1995). Tissue-specific expression of a FMR1/beta-galactosidase fusion gene in transgenic mice. Hum. Mol. Genet. *4*, 359–366.

Hinton, V.J., Brown, W.T., Wisniewski, K., and Rudelli, R.D. (1991). Analysis of neocortex in three males with the fragile X syndrome. Am. J. Med. Genet. *41*, 289–294.

Irwin, S.A., Galvez, R., and Greenough, W.T. (2000). Dendritic spine structural anomalies in fragile-X mental retardation syndrome. Cereb. Cortex *10*, 1038–1044.

Irwin, S.A., Patel, B., Idupulapati, M., Harris, J.B., Crisostomo, R.A., Larsen, B.P., Kooy, F., Willems, P.J., Cras, P., Kozlowski, P.B., et al. (2001). Abnormal dendritic spine characteristics in the temporal and visual cortices of patients with fragile-X syndrome: a quantitative examination. Am. J. Med. Genet. *98*, 161–167.

Kutsche, K., Yntema, H., Brandt, A., Jantke, I., Nothwang, H.G., Orth, U., Boavida, M.G., David, D., Chelly, J., Fryns, J.P., et al. (2000). Mutations in ARHGEF6, encoding a guanine nucleotide exchange factor for Rho GTPases, in patients with X-linked mental retardation. Nat. Genet. *26*, 247–250.

Lee, T., and Luo, L. (1999). Mosaic analysis with a repressible neurotechnique cell marker for studies of gene function in neuronal morphogenesis. Neuron *22*, 451–461.

Lee, C.G., Bae, K.H., and Edery, I. (1998). The *Drosophila* CLOCK protein undergoes daily rhythms in abundance, phosphorylation, and interactions with the PER-TIM complex. Neuron *21*, 857–867.

Levine, J.D., Casey, C.I., Kalderon, D.D., and Jackson, F.R. (1994). Altered circadian pacemaker functions and cyclic AMP rhythms in the *Drosophila* learning mutant *dunce*. Neuron *13*, 967–974.

Levine, J.D., Funes, P., Dowse, J.B., and Hall, J.C. (2002). Signal analysis of behavioral and molecular cycles. BMC Neurosci. *3*, 1–25.

Lugenbeel, K.A., Peier, A.M., Carson, N.L., Chudley, A.E., and Nelson, D.L. (1995). Intragenic loss of function mutations demonstrate the primary role of FMR1 in fragile X syndrome. Nat. Genet. *10*, 483–485.

Meijer, H., de Graaff, E., Merckx, D.M., Jongbloed, R.J., de Die-Smulders, C.E., Engelen, J.J., Fryns, J.P., Curfs, P.M., and Oostra, B.A. (1994). A deletion of 1.6 kb proximal to the CGG repeat of the FMR1 gene causes the clinical phenotype of the fragile X syndrome. Hum. Mol. Genet. *3*, 615–620.

Morton, J.E., Bundey, S., Webb, T.P., MacDonald, F., Rindl, P.M., and Bullock, S. (1997). Fragile X syndrome is less common than previously estimated. J. Med. Genet. *34*, 1–5.

Newby, L.M., White, L., DiBartolomeis, S.M., Walker, B.J., Dowse, H.B.J., Ringo, M., Khuda, N., and Jackson, F.R. (1991). Mutational analysis of the *Drosophila miniature-dusky (m-dy)* locus: Effects on cell size and circadian rhythms. Genetics *128*, 571–582.

Nimchinsky, E.A., Oberlander, A.M., and Svoboda, K. (2001). Abnormal development of dendritic spines in FMR1 knock-out mice. J. Neurosci. *21*, 5139–5146.

O'Brien, G. (2000). Behavioural phenotypes. J. R. Soc. Med. *93*, 618–620.

Park, J.H., Helfrich-Forster, C., Lee, G., Liu, L., Rosbash, M., and Hall, J.C. (2000). Differential regulation of circadian pacemaker output by separate clock genes in Drosophila. Proc. Natl. Acad. Sci. USA *97*, 3608–3613.

Peier, A.M., McIlwain, K.L., Kenneson, A., Warren, S.T., Paylor, R., and Nelson, D.L. (2000). (Over)correction of FMR1 deficiency with YAC transgenics: behavioral and physical features. Hum. Mol. Genet. *9*, 1145–1159.

Pieretti, M., Zhang, F.P., Fu, Y.H., Warren, S.T., Oostra, B.A., Caskey, C.T., and Nelson, D.L. (1991). Absence of expression of the FMR-1 gene in fragile X syndrome. Cell *66*, 817–822.

Renn, S.C., Park, J.H., Rosbash, M., Hall, J.C., and Taghert, P.H. (1999). A pdf neuropeptide gene mutation and ablation of PDF neurons each cause severe abnormalities of behavioral circadian rhythms in Drosophila. Cell *99*, 791–802.

Rudelli, R.D., Brown, W.T., Wisniewski, K., Jenkins, E.C., Laure-Kamionowska, M., Connell, F., and Wisniewski, H.M. (1985). Adult fragile X syndrome. Clinico-neuropathologic findings. Acta Neuropathol. (Berl.) *67*, 289–295.

Siomi, H., Siomi, M.C., Nussbaum, R.L., and Dreyfuss, G. (1993). The protein product of the fragile X gene, FMR1, has characteristics of an RNA-binding protein. Cell *74*, 291–298.

Tamanini, F., Willemsen, R., van Unen, L., Bontekoe, C., Galjaard, H., Oostra, B.A., and Hoogeveen, A.T. (1997). Differential expression of FMR1, FXR1 and FXR2 proteins in human brain and testis. Hum. Mol. Genet. *6*, 1315–1322.

Turner, G., Webb, T., Wake, S., and Robinson, H. (1996). Prevalence of fragile X syndrome. Am. J. Med. Genet. *64*, 196–197.

Van Vactor, D.V., and Lorenz, L.J. (1999). Neural development: The semantics of axon guidance. Curr. Biol. *9*, R201–R204.

Verkerk, A.J., Pieretti, M., Sutcliffe, J.S., Fu, Y.H., Kuhl, D.P., Pizzuti, A., Reiner, O., Richards, S., Victoria, M.F., Zhang, F.P., et al. (1991). Identification of a gene (FMR-1) containing a CGG repeat coincident with a breakpoint cluster region exhibiting length variation in fragile X syndrome. Cell *65*, 905–914.

Wan, L., Dockendorff, T.C., Jongens, T.A., and Dreyfuss, G. (2000). Characterization of dfxr, a Drosophila melanogaster homolog of the fragile X mental retardation protein. Mol. Cell. Biol. *20*, 8536–8547.

Wisniewski, K.E., Segan, S.M., Miezejeski, C.M., Sersen, E.A., and Rudelli, R.D. (1991). The Fra(X) syndrome: neurological, electrophysiological, and neuropathological abnormalities. Am. J. Med. Genet. *38*, 476–480.

Wittwer, F., van der Straten, A., Keleman, K., Dickson, B.J., and Hafen, E. (2001). Lilliputian: an AF4/FMR2-related protein that controls cell identity and cell growth. Development *128*, 791–800.

Zhang, Y.Q., Bailey, A.M., Matthies, H.J., Renden, R.B., Smith, M.A., Speese, S.D., Rubin, G.M., and Broadie, K. (2001). Drosophila fragile X-related gene regulates the MAP1B homolog futsch to control synaptic structure and function. Cell *107*, 591–603.